

Path planning for light-induced dielectrophoretic manipulation of micro-particles

Chang Yan Zhu Xiaolu Ni Zhonghua

(School of Mechanical Engineering, Southeast University, Nanjing 211189, China)

(Jiangsu Key Laboratory for Design and Manufacture of Micro-Nano Biomedical Instruments, Southeast University, Nanjing 211189, China)

Abstract: To realize automatic manipulation of micro-particles by light-induced dielectrophoresis (LDEP), a path-planning scheme based on the improved artificial potential field (APF) for micro light pattern movements is proposed. An algorithm combining guided target and point obstacle based on a new local minimum judging criterion is specially designed, which can solve the local minimum problems encountered by the traditional APF. Experiments of real-time particle manipulation based on this algorithm are implemented and the experimental results show that the proposed approach can overcome the local minimum problems of the traditional APF method, and it is validated to be highly stable for intensive particle obstacles during LDEP manipulation. Consequently, this method can realize real-time manipulation of micro-nano particles with safety, decrease the difficulty of manual manipulation, and thus improve the efficiency of manipulation of micro-particles.

Key words: light-induced dielectrophoresis; artificial potential field; guided target; point obstacle

doi: 10.3969/j.issn.1003-7985.2011.04.009

In recent years, it has become possible to realize flexible manipulation of micro-nano particles with the development of light-induced dielectrophoresis (LDEP)^[1-3]. The basic principle of LDEP^[4] is that the photoconductive material in the LDEP device has a much higher conductivity under illumination than that without illumination. Due to different partial voltages between bright areas and dark areas, a non-uniform electric field in the manipulation space is formed and thus the LDEP force is produced, which can be used to achieve the dielectric manipulation of micro-nano particles. Since LDEP is employed in the micro-manipulation research area, it is easy to dynamically manipulate particles in a non-contact mode by controlling the light-induced virtual electrode, which is generated by digital micro-mirror device display technology^[2]. The typical structure of the light-induced virtual electrode is ring-like. The micro-particle is trapped by the LDEP force generated by the annular light-induced virtual electrode, so synchronous motion between the trapped particle and the ring electrode can be achieved. Because the light-induced virtual electrode can

transport particles from one position to another position, it can be imaged as a “robot” formed by a light pattern. So we call it a light robot in this paper instead. However, the LDEP manipulation usually needs an operator to control the complex motion of the micro light patterns during the whole operating process^[5-7], which is labor-consuming. In order to realize automatic LDEP manipulation, a real-time path planning algorithm for light robots is crucially needed to be integrated in the commonly used micro-nano particles manipulation platform based on LDEP^[8-9].

Path planning methods can be divided into traditional methods and intelligent methods^[10]. Intelligent methods include fuzzy logic^[11], neural networks^[12] and the GA algorithm^[13]. The intelligent methods usually have complex models and require much more iterations to achieve the optimal path which usually results in huge computation. So the intelligent methods are not suitable for the real-time control of the automatic manipulation of micro-particles. Additionally, there are mainly three traditional methods^[10] available: V-graph, the grid method, and artificial potential field (APF). The APF method was put forward by Khatib^[14], which is widely used due to the concise expression and good real-time performance. As a heuristic method, a virtual potential field is defined in C space^[15], which will make the target attract the moving object, while the obstacles repel it. In this way, the moving object will head for the goal in the direction of a negative gradient of the total potential. But there is a local minimum problem which will trap the moving object before reaching its goal.

Thus, it is the crucial bottleneck of the APF method to avoid the local minimum problem. Ge and Cui^[16] proposed a modified repulsive potential function taking target and obstacles into consideration, and it effectively solves the local minimum problem that the obstacle is close to the goal. Zhang et al.^[17] brought simulated annealing into the APF method. Its basic idea is that the robot moves forwards in the direction of higher potential with a certain probability, but there are still many shock points on the final path. Kuang and Wang^[18] combined the APF method with the GA algorithm, and the GA algorithm is used to obtain the optimal parameters for the APF approach, but its real-time performance is not good due to the large amounts of calculation.

In this paper, an improved APF based path planning method for light robots is proposed and implemented in the LDEP manipulation. First, a new local minimum judging criterion is given. Then, based on the criterion, an algorithm which combines the guided target and the point obstacle concept is designed to avoid local minimums. Finally, the proposed approach is practically applied to a micro-nano

Received 2011-07-26.

Biographies: Chang Yan (1986—), male, graduate; Ni Zhonghua (corresponding author), male, doctor, professor, nzh2003@seu.edu.cn.

Foundation items: The National Natural Science Foundation of China (No. 91023024, 51175083), Scientific Research Foundation of Graduate School of Southeast University (No. YBJJ1020), Jiangsu Graduate Innovative Research Program (No. CX10B_062Z).

Citation: Chang Yan, Zhu Xiaolu, Ni Zhonghua. Path planning for light-induced dielectrophoretic manipulation of micro-particles [J]. Journal of Southeast University (English Edition), 2011, 27(4): 388 – 393. [doi: 10.3969/j.issn.1003-7985.2011.04.009]

bio-particles manipulation platform based on LDEP using Visual C++. Experiments show that the proposed approach can realize real-time manipulation of micro-particles with safety, decrease the difficulty of the manual manipulation, and thus improve the efficiency of the manipulation of micro-particles.

1 Modified APF Model

In the micro-scaled manipulation workspace, multiple particles can be trapped using the same number of light robots. It means that when a single particle is driven toward a specific target, the other light robots should be viewed as obstacles. The basic idea of the APF method is that the light robot, obstacles and the target are simplified into geometric points. The light robot heads for the target and moves under the artificial force, while the obstacles repulse the moving light robot and the target attracts the light robot. So the light robot moves in the direction of the composite force.

The attractive potential function is defined as

$$U_{\text{att}}(\mathbf{q}) = \frac{1}{2} \xi \rho^m(\mathbf{q}, \mathbf{q}_{\text{goal}}) \quad (1)$$

where $\rho(\mathbf{q}, \mathbf{q}_{\text{goal}}) = \|\mathbf{q}_{\text{goal}} - \mathbf{q}\|$ represents the distance between the light robot and the target; ξ is a positive proportional coefficient; m is equal to 2.

The attractive force is the negative gradient of the attractive potential, which is defined as

$$\mathbf{F}_{\text{att}}(\mathbf{q}) = -\nabla U_{\text{att}}(\mathbf{q}) = \xi(\mathbf{q}_{\text{goal}} - \mathbf{q}) \quad (2)$$

The modified repulsive potential function^[16] is defined as

$$U_{\text{rep}}(\mathbf{q}) = \begin{cases} \frac{1}{2} \eta \left(\frac{1}{\rho(\mathbf{q}, \mathbf{q}_{\text{obs}})} - \frac{1}{\rho_0} \right)^2 \rho^n(\mathbf{q}, \mathbf{q}_{\text{goal}}) & \rho(\mathbf{q}, \mathbf{q}_{\text{obs}}) \leq \rho_0 \\ 0 & \rho(\mathbf{q}, \mathbf{q}_{\text{obs}}) > \rho_0 \end{cases} \quad (3)$$

where η is a positive proportional coefficient; $\rho(\mathbf{q}, \mathbf{q}_{\text{obs}})$ is the shortest distance between the light robot and obstacles; ρ_0 is the effect distance of obstacles; n is any positive real number. In this study, ρ_0 is equal to the diameter of the light robot, and n is equal to 2.

The corresponding repulsive force is

$$\mathbf{F}_{\text{rep}}(\mathbf{q}) = -\nabla U_{\text{rep}}(\mathbf{q}) = \begin{cases} \mathbf{F}_{\text{rep1}} \mathbf{n}_{\text{OR}} + \mathbf{F}_{\text{rep2}} \mathbf{n}_{\text{RG}} & \rho(\mathbf{q}, \mathbf{q}_{\text{obs}}) \leq \rho_0 \\ 0 & \rho(\mathbf{q}, \mathbf{q}_{\text{obs}}) > \rho_0 \end{cases} \quad (4)$$

where

$$\begin{aligned} \mathbf{F}_{\text{rep1}} &= \eta \left(\frac{1}{\rho(\mathbf{q}, \mathbf{q}_{\text{obs}})} - \frac{1}{\rho_0} \right) \frac{\rho^n(\mathbf{q}, \mathbf{q}_{\text{goal}})}{\rho^2(\mathbf{q}, \mathbf{q}_{\text{obs}})} \\ \mathbf{F}_{\text{rep2}} &= \frac{n}{2} \eta \left(\frac{1}{\rho(\mathbf{q}, \mathbf{q}_{\text{obs}})} - \frac{1}{\rho_0} \right)^2 \rho^{n-1}(\mathbf{q}, \mathbf{q}_{\text{goal}}) \\ \mathbf{n}_{\text{OR}} &= \nabla \rho(\mathbf{q}, \mathbf{q}_{\text{obs}}), \quad \mathbf{n}_{\text{RG}} = -\nabla \rho(\mathbf{q}, \mathbf{q}_{\text{goal}}) \end{aligned}$$

\mathbf{n}_{OR} and \mathbf{n}_{RG} are two unit vectors from the obstacle pointing to the light robot and from the light robot pointing to the target, respectively.

The resultant force on the light robot is

$$\mathbf{F}_{\text{Total}} = \mathbf{F}_{\text{att}} + \mathbf{F}_{\text{rep}} \quad (5)$$

And it determines the current direction of the light robot, known as heading angle α .

1.1 Criterion for judging local minimums

Because the light robot always moves forwards in the direction of the negative gradient, a successful path must contain a series of points where the total potential always decreases, and at the goal position the total potential has the minimum. Fig. 1(a) shows the equipotential field curves of a typical obstacle environment calculated by the modified APF. The light robot heads for the target from S to G , and the total potential stops decreasing while the light robot reaches the internal area of the U-shape obstacle. Due to the pixel level precision for the light robot motion, the light robot will shock between two neighboring path points. In this case, the value of the total potential will be high and low circularly, as shown in Fig. 1(b).

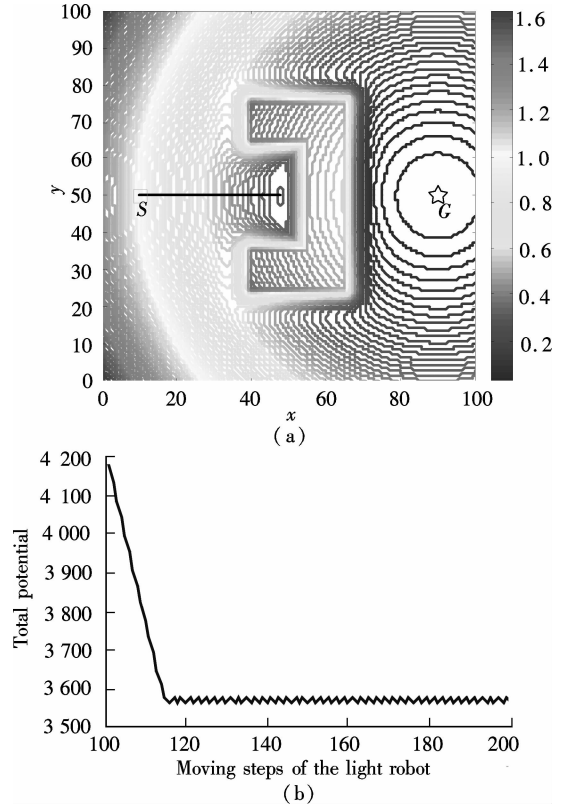


Fig. 1 Typical U-shaped obstacle environment. (a) Curve of equipotential field; (b) Partial curve of total potential

Hereby, the new criterion of local minimums is proposed as follows: The total potential of current time is denoted as $U_c(t)$, and the total potential of next time is denoted as $U_c(t+T_0)$. If $U_c(t+T_0) - U_c(t) > \Delta$, the light robot is regarded to be trapped in local minimums, where T_0 is the sample interval of total potential and Δ is a nonnegative constant called sensitivity of potential. The smaller the Δ , the higher the sensitivity of potential.

1.2 Guided target and point obstacle

Based on the above criterion, an algorithm combining the guided target and the point obstacle is proposed to solve the local minimum problem.

For simplification, the light robot which traps micro-particles can be regarded as a mass point, and thus the size of obstacles should be transformed from the work space to C space^[15].

Suppose S and G represent the initial position and the goal of the light robot, respectively; α is the heading angle from S to G ; P is the local minimum position, which is set as the circle center of the detection area, and R_o is the search radius. Then the obstacles located at the angular region of $[-\pi/2 + \alpha, \pi/2 + \alpha]$ can be searched, as shown in Fig. 2(a).

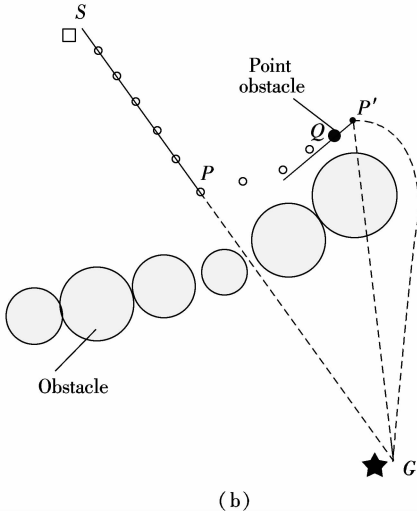
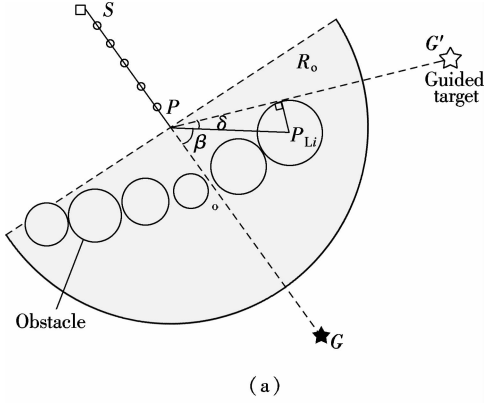


Fig. 2 Schematic of escaping from local minimums. (a) Setup of guided target; (b) Setup of point obstacle

Let $ObsL$ be a set containing the searched obstacles in the left search area. $ObsL = \{O_{L1}, O_{L2}, \dots, O_{Lm}\}$. The center of O_{Li} is P_{Li} and the radius is R_{Li} ; m is the number of obstacles. Similarly, another set named $ObsR$ can be easily defined just by replacing “L” with “R”.

1.2.1 Setup of guided target

Suppose S_L and S_R to be the sum area of obstacles in $ObsL$ and $ObsR$, respectively. If $S_L \leq S_R$, it means that the threat of obstacles in the left search area is smaller than that in the right one; thus, the guided target should be set in the direction of the left search area. Otherwise, it should be set in the direction of the right search area.

Taking into account the situation of $S_L \leq S_R$, as shown in Fig. 2(a), O_{Li} is the obstacle in $ObsL$ which is the farthest from the direction of heading angle α . The greatest included angle is β , so the guided target direction ϕ is

$$\phi = \alpha + (\beta + \delta) \quad (6)$$

where $\beta = \angle(PG, PP_{Li})$, $\delta = \arcsin \frac{R_{Li}}{\|P_{Li}P\|}$.

Similarly, if $S_L > S_R$, O_{Rj} is the obstacle in $ObsR$ which is the farthest from the direction of heading angle α , and the greatest included angle is β .

The guided target direction ϕ is

$$\phi = \alpha - (\beta + \delta) \quad (7)$$

where $\beta = \angle(PG, PP_{Rj})$, $\delta = \arcsin \frac{R_{Li}}{\|P_{Rj}P\|}$.

The guided target is supposed as $G'(x, y)$, which can be obtained as

$$\begin{cases} x_{G'} = x_P + M \cos \phi \\ y_{G'} = y_P + M \sin \phi \end{cases} \quad (8)$$

where M is the Euclidean distance between the guided target and the local minimum position P . If M is very small, the light robot will reach the guided target before escaping from the local minimum completely. So M is usually assigned to the maximum scale of the manipulation space.

While the light robot heads for the guided target, the global target must be reset to the real target promptly, otherwise the length of path will increase greatly. Let d_{\min} be the shortest distance between the light robot and all obstacles. When $d_{\min} > \rho_0$, the global target should be reset to G immediately.

1.2.2 Setup of point obstacle

In order to avoid the shocking between P' and P in complex obstacle environments such as U-shaped obstacles, a point obstacle concept is put forward to overcome the potential risk of rolling back in this study.

Suppose at time t_c , the global target is reset to the real goal G , as shown in Fig. 2(b). P' is the current position of the light robot, that is $P' = X(t_c)$, so point obstacle Q is set as

$$Q = X(t_c - t) \quad (9)$$

where t is the delay time.

By adding the point obstacle to the manipulation space, the light robot will be repulsed from rolling back.

1.3 Modified APF for light robot

As the typically used shape of light robots is ring-like, the structure of the light robot in the algorithm is selected to be ring-like. Besides, the radius of the light robot in the algorithm is set as an external radius for safety, and the radii of other types of light robots such as square or diamond can be equivalent to the radii of their circumcircles. Fig. 3 shows the flow chart of the improved APF approach for the light robot. The improved APF approach based on the guided target and the point obstacle is given as follows:

Step 1 The micro-nano particles manipulation platform is initialized. Suppose that $VectorL$ and $VectorR$ represent the times of the light robot turning to the left and the right sides, respectively, when a local minimum occurs. The initial values of both $VectorL$ and $VectorR$ are zero.

Step 2 Trap the particle of interest using a ring-like light robot and set the target G .

Step 3

a) The light robot moves forwards according to the heading angle α computed by Eq. (5). If $U_C(t + T_0) - U_C(t) > \Delta$, then go to Step 4.

b) If the guided target G' is set up, detect the shortest distance d_{\min} between the light robot and all the obstacles. If $d_{\min} > \rho_0$, then reset the global target to G , add the point obstacle according to Eq. (9), and $\text{VectorL} = \text{VectorR} = 0$, go to a).

c) If the light robot reaches the real target, then the algorithm stops; otherwise go to a).

Step 4

a) Set the current position of the light robot as the circle center of the detection area, and R_0 as the search radius. Then find the obstacles which are located at the angular region of $[-\pi/2 + \alpha, \pi/2 + \alpha]$.

b) Compute guided target direction ϕ .

If $\text{VectorL} = \text{VectorR} = 0$ and $S_L \leq S_R$ then Eq. (6) should be used, and VectorL plus 1;

If $\text{VectorL} = \text{VectorR} = 0$ and $S_L > S_R$ then Eq. (7) should be used, and VectorR plus 1;

If $\text{VectorL} > 0$ then Eq. (6) should be used;

If $\text{VectorR} > 0$ then Eq. (7) should be used.

c) Compute the guided target G' according to Eq. (8), replace the global target with G' , and go to Step 3.

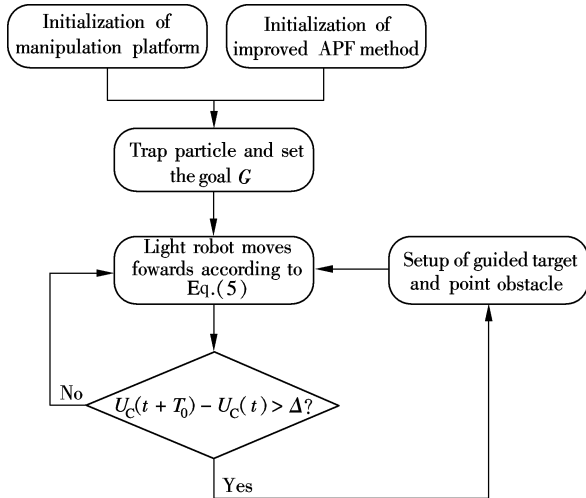


Fig. 3 Flow chart of the improved APF approach for light robot

2 Experimental Verification

In order to achieve automatic manipulation of micro-particles, the micro-nano particles manipulation platform is made up of a projection module and a vision module. The projection module includes several optical lenses and a high accuracy DLP projector by which the light-induced virtual electrode (light robot) is generated. When the light robot is projected on the chip of LDEP through a series of optical components, the visual feedback will be done simultaneously by the vision module consisting of a CCD camera and a biological microscope, as shown in Fig. 4.

To validate the algorithm, experiments of real-time manipulation of standard particles are performed. The polystyrene particles used in the experiment are bought from Duke Scientific Corporation and have a diameter of about $30 \mu\text{m}$.

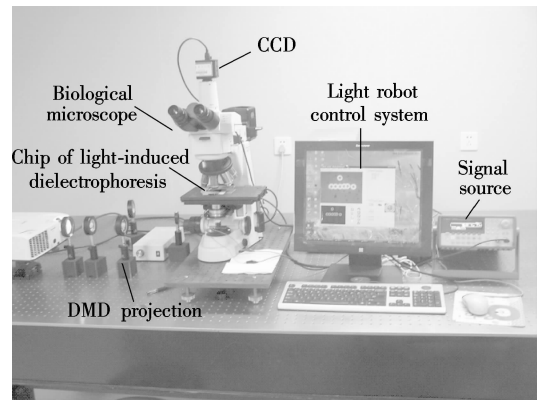


Fig. 4 Micro-nano particles manipulation platform

The particles are injected into the LDEP device^[19] in which deionized water is used as a buffer solution. Then, a signal with a peak-peak value of 20 V and a frequency of 1 MHz is applied to the LDEP device.

Fig. 5 and Fig. 6 show the manipulation of a single particle in linear obstacles and U-shaped obstacles, respectively. As shown in Fig. 5 and Fig. 6, S and G represent the initial position and the target, respectively, and the dashed circles signify the position of the light robot which traps the particle. The internal diameter and the external diameter of the light robot are 65 and $120 \mu\text{m}$, respectively. And the speed of the light robot is about $15 \mu\text{m/s}$. Fig. 5(f) and Fig. 6(f) show the trajectory of the light robot.

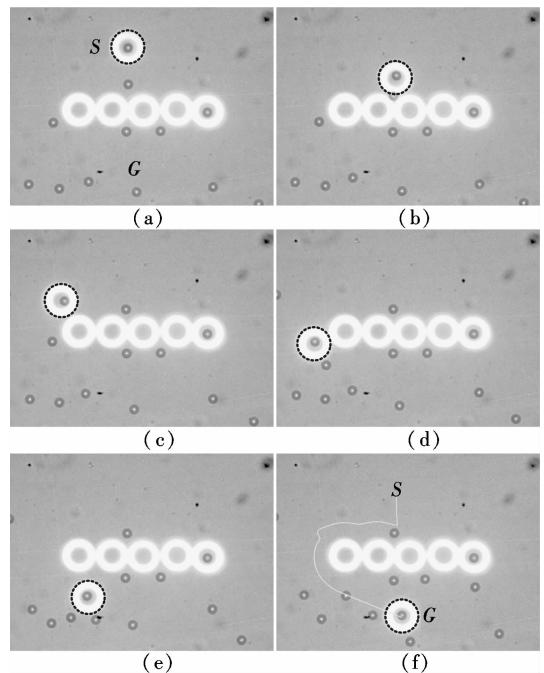


Fig. 5 A series of images for single particle manipulation in linear obstacles environment

If the traditional APF method is used, the light robot will be trapped at the local minimum position in experiment 1 as shown in Fig. 5(b) as well as the position in experiment 2 as shown in Fig. 6(b). In this case, the particle cannot be transported to the target.

Moreover, by using the improved APF approach, the light robot will automatically follow the wall composed of obstacles while there is more than one local minimum posi-

tion. In experiment 2, the light robot turned right twice at local minimums before reaching its goal (see Fig. 6). Compared with Ref. [20], the proposed method only needs two variables (namely VectorL and VectorR as mentioned in section 1.3) to realize the wall-following motion.

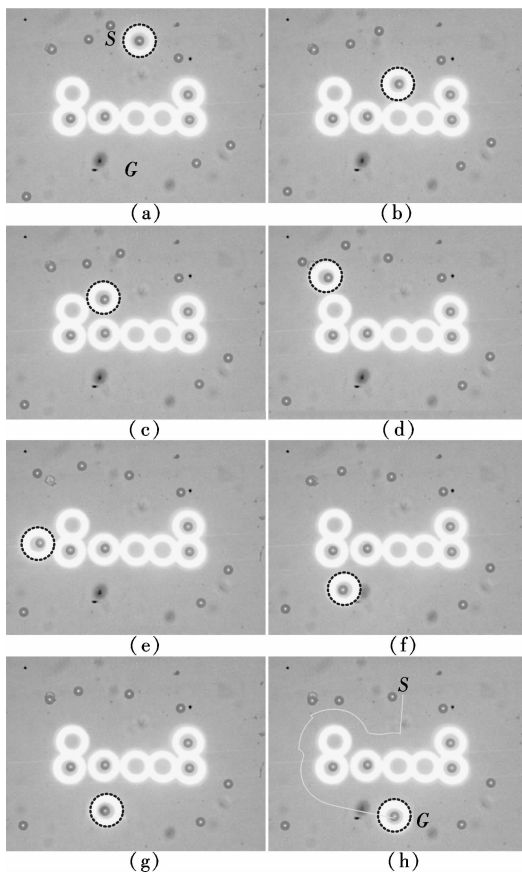


Fig. 6 A series of images for single particle manipulation in U-shaped obstacles environment

Fig. 7 and Fig. 8 show the trajectories of both the light robot and the transported particle in two experiments, respectively. It is obvious that the trajectory of the transported particle is almost coinciding with that of the light robot. We can see that the particle moves along with the light robot without being lost. The experimental results show that the algorithm can meet the requirements of safety and stability.

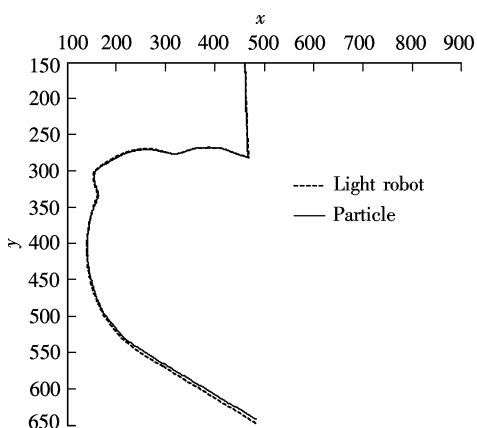


Fig. 7 Trajectory of particle and light robot for single particle manipulation in linear obstacles environment

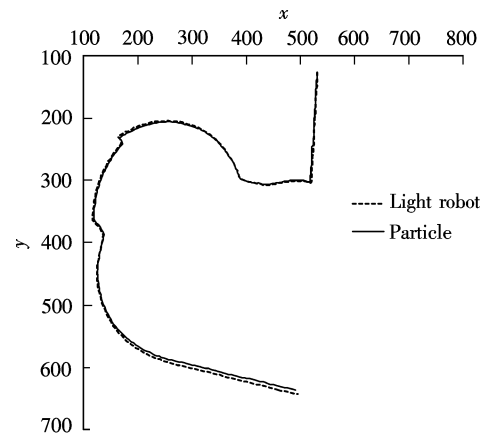


Fig. 8 Trajectory of particle and light robot for single particle manipulation in U-shaped obstacles environment

3 Conclusion

This study proposes an improved artificial potential field-based path planning method for a light-induced virtual electrode named a light robot, which is used to manipulate particles in a non-contact mode by LDEP. For the local minimum problem, a new local minimum criterion is given. Based on the new criterion, an algorithm combining the guided target and the point obstacle concept is given to solve the local minimum problem. As a result, the algorithm does not need iterative computation and improves real-time performance of micro-manipulation. Furthermore, the light robot control system based on the above algorithm is built up, and the experiments of real-time manipulation show that the algorithm is validated to be highly stable for intensive obstacles. Consequently, this method can realize real-time manipulation of micro-nano particles with safety and stability, and thus improve the efficiency of the manipulation of micro-particles.

References

- [1] Hughes M P. Strategies for dielectrophoretic separation in laboratory-on-a-chip systems [J]. *Electrophoresis*, 2002, **23**(16): 2569 – 2582.
- [2] Chiou P Y, Ohta A T, Wu M C. Massively parallel manipulation of single cells and microparticles using optical images [J]. *Nature*, 2005, **436**(7049): 370 – 372.
- [3] Jamshidi A, Neale S L, Yu K, et al. NanoPen: dynamic, low-power, and light-actuated patterning of nanoparticles [J]. *Nano Lett*, 2009, **9**(8): 2921 – 2925.
- [4] Song C F, Yi H, Ni Z H. Single micro-particle manipulation based on light-induced dielectrophoresis [J]. *Journal of Mechanical Engineering*, 2010, **46**(7): 148 – 153.
- [5] Hwang H, Choi Y J, Choi W, et al. Interactive manipulation of blood cells using a lens-integrated liquid crystal display based optoelectronic tweezers system [J]. *Electrophoresis*, 2008, **29**(6): 1203 – 1212.
- [6] Hwang H, Oh Y, Kim J J, et al. Reduction of nonspecific surface-particle interactions in optoelectronic tweezers [J]. *Appl Phys Lett*, 2008, **92**(2): 024108.
- [7] Hwang H, Park Y H, Park J K. Optoelectrofluidic control of colloidal assembly in an optically induced electric field [J]. *Langmuir*, 2009, **25**(11): 6010 – 6014.
- [8] Ni Z H, Yi H, Zhu S C. Research on critical technology of micro/nano bioparticles manipulation platform based on

- light-induced dielectrophoresis [J]. *Sci China Ser E: Tech Sci*, 2009, **39**(10): 1635 – 1642.
- [9] Zhu X L, Yi H, Ni Z H. Frequency-dependent behaviors of individual microscopic particles in an optically induced dielectrophoresis device [J]. *Biomicrofluidics*, 2010, **4**(1): 013202.
- [10] Zhang Y, Wu C D, Yuan B L. Progress on path planning research for robot [J]. *Control Engineering of China*, 2003, **10**(Z1): 152 – 154. (in Chinese)
- [11] Aydin S, Temeltas H. Fuzzy-differential evolution algorithm for planning time-optimal trajectories of a unicycle mobile robot on a predefined path [J]. *Adv Robotics*, 2004, **18**(7): 725 – 748.
- [12] Yu J L, Cheng S Y, Sun Z Q. An optimal algorithm of 3D path planning for mobile robots [J]. *Journal of Central South University*, 2009, **40**(2): 471 – 477.
- [13] Ali M S A D, Babu N R, Varghese K. Collision free path planning of cooperative crane manipulators using genetic algorithm [J]. *J Comput Civil Eng*, 2005, **19**(2): 182 – 193.
- [14] Khatib O. Real-time obstacle avoidance for manipulators and mobile robots [J]. *Int J Robot Res*, 1986, **5**(1): 90 – 98.
- [15] de Berg M, Cheong O, van Kreveld M, et al. *Computational geometry: algorithms and applications* [M]. 3rd Ed. Springer-Verlag, 2008: 284 – 287.
- [16] Ge S S, Cui Y J. New potential functions for mobile robot path planning [J]. *IEEE Transactions on Robotics and Automation*, 2000, **16**(5): 615 – 620.
- [17] Zhang P Y, Lu T S, Song L B. Soccer robot path planning based on the artificial potential field approach with simulated annealing [J]. *Robotica*, 2004, **22**(5): 563 – 566.
- [18] Kuang F, Wang Y N. Robot path planning based on hybrid artificial potential field/genetic algorithm [J]. *Journal of System Simulation*, 2006, **18**(3): 774 – 777. (in Chinese)
- [19] Zhu X L, Yin Z F, Gao Z Q. Experimental study on filtering, transporting, concentrating and focusing of microparticles based on optically induced dielectrophoresis [J]. *Sci China Ser E: Tech Sci*, 2010, **53**(9): 2388 – 2396.
- [20] Zhu Y, Zhang T, Song J Y. An improved wall following method for escaping from local minimum in artificial potential field based path planning [C]// *Joint 48th IEEE Conference on Decision and Control and 28th Chinese Control Conference*. Shanghai, China, 2009: 6017 – 6022.

基于光诱导介电泳的微粒子操纵路径规划方法

常 严 朱晓璐 倪中华

(东南大学机械工程学院, 南京 211189)

(东南大学江苏省微纳生物医疗器械设计与制造重点实验室, 南京 211189)

摘要:为实现基于光诱导介电泳的微粒子自动化操纵,设计了基于改进人工势场的缩微光图案路径规划方法.针对传统人工势场的局部极小问题,给出一种新的局部极小判别准则.在此基础上提出导引目标和点障碍相结合的方法来脱离局部极小点,并将改进后的人工势场算法集成于基于光诱导介电泳的微纳米生物粒子操纵平台中,进行微粒子操纵实验.结果表明,该方法充分发挥了势场法的优势,对密集障碍环境稳定性强,能够实现微纳米粒子的安全实时操纵,从而降低了人工操纵难度,提高了微操纵效率.

关键词:光诱导介电泳;人工势场;导引目标;点障碍

中图分类号: TP271